Jurnal Kimia Valensi, Vol 9(1), May 2023, 13-21
Available online at Website: http://journal.uinjkt.ac.id/index.php/valensi

Zeolite from Zirconium-Modified Fly Ash Waste for Absorption of Phosphate Compounds in Waters

Mu'izzah Irsyadi Putri, Asep Saefumillah, Ridla Bakri

Department of Chemistry, Faculty of Mathematics and Natural Sciences, University of Indonesia, Jl. Lingkar Kampus Raya, Pondok Cina, Beji, Depok, Jawa Barat 16424, Indonesia.

**Corresponding author: asep.saefumillah@sci.ui.ac.id*

Received: July 2022; Revision: September 2022; Accepted: October 2022; Available online: May 2023

Abstract

Eutrophication is a phenomenon of decreasing air quality caused by the very high amount of phosphate ions in the aquatic system. Thus, an effective and efficient adsorbent is needed for phosphate absorption in aquatic systems. In this study, zeolit from fly ash waste was modified with zirconium (Zr) as an adsorbent for phosphate absorption in aquatic systems. Fly ash was pretreated with acid and then synthesised using the hydrothermal method. And then, the results of the fly ash zeolit synthesis were continued using zirconium. The adsorption capacity was tested through several parameters, including the adsorbent concentration test, variations in pH,and contact time. Zirconium-modified zeolite (ZrMZ) adsorbent was the most effective adsorbent for phosphate adsorption, with an adsorption capacity of 3.015 mg-P/g at a 3 g/L adsorbent dosage and pH 7. The adsorption kinetics for the ZrMZ adsorbent followed pseudo-second-order kinetics. The best result of ZrMZ adsorbent to absorb phosphate in lake water was an adsorption capacity value of 0.186 mg-P/g and an adsorption efficiency of 81.137%.

Keywords: Adsoption; fly ash; phosphate; zeolite; zirconium.

DOI: *10.15408/jkv.v9i1.26951*

1. INTRODUCTION

The process of eutrophication in aquatic systems is caused by a significant increase in the quantity of nutrients, such as excessive phosphorus (P), in the water, which can cause disruption, damage, and danger to aquatic organisms (Sasongko *et al.*, 2014). Phosphate in water is naturally derived from the decomposition, weathering, and degradation of vegetation and dead organisms. Increasing phosphate levels can impact the growth and metabolism of phytoplankton and aquatic plants, resulting in algal blooms (Patty, 2014; Simbolon, 2016). The method of phosphate adsorption with minerals is regarded as an effective and easy technique for phosphate absorption in water. Zeolites are widely used in phosphate adsorption processes today. It is due to zeolite has a large surface area and is selective in the adsorption process (Jumaeri *et al.*, 2013).

Zeolite synthesis based on fly ash waste from coal combustion is widely developed for adsorbents in phosphate absorption in water system (Faradilla *et al.,* 2016). It is due to fly ash waste is quite vast and has an impact on generating severe environmental contamination. Goscianska *et al.* (2018) demonstrated 58.2 mg/g phosphate adsorption capacity using fly ash-based zeolite modified with lanthanum for phosphate removal in water. Fly ash waste treated with magnetite (Fe_3O_4) was employed by Zahrah *et al.* (2020) to remove phosphate from aquatic systems with an adsorption capacity of 2.24 mg-P/g and an efficiency of 90.42%. Due to the presence of several active sites on the surface of zirconium-modified zeolite, the amount of adsorbed phosphate grows quickly at the beginning of the phosphate adsorption process (Xiong *et al.*, 2017).

Ma *et al.* (2019), who added zirconium (Zr) to zeolite-Y to increase phosphate adsorption, demonstrated that zirconium (Zr) can be employed as an adsorbent in phosphate sorption with a variety of modifications. A Zr-modified chitosan-zeolite is also used to remove Vanadium (V) ions from water along with phosphate (Rodrigues *et al.,* 2012; Salehi *et al.,* 2020). Hard, heat- and acid-resistant, and

P-ISSN: 2460-6065, E-ISSN: 2548-3013

corrosion-resistant metal element Zr has a stable hexagonal crystal structure (HCP). Despite being highly accessible and rarely used in nature, Zr is nonetheless widely used (Poernomo *et al.*, 2016). Zirconium-based oxides (zirconium oxide and hydrous zirconium oxide) have attracted a lot of interest for application as adsorbents for phosphorus removal in aquatic systems because they are chemically stable, non-toxic, insoluble in water, and have a good affinity for phosphate in water (Yang *et al.*, 2015).

This study aims to produce zeolite from waste fly ash, which will subsequently be altered with zirconium (Zr). Fly ash zeolite that has been treated with zirconium was employed as an adsorbent in aquatic systems to absorb phosphate. In order to conduct the analysis, it was necessary to examine the effects of changing the adsorbent amount, pH, temperature, contact time, and phosphate concentration. Using zirconium-modified fly ash zeolite as an adsorbent, successful phosphate sorption outcomes were attained. This research is urgent because it aims to use fly ash, a byproduct of burning coal, as an adsorbent. In order to measure the amount of phosphate in water bodies and avoid eutrophication occurrences. This study is also planned to provide information about the synthesis of zeolite from waste zirconium-modified fly ash.

2. MATERIALS AND METHODS

Materials and Tools

Fly ash from PT Sinar Mas Agro Recources and Technology (SMART Tbk) with a total SiO_2, Al_2O_3, and Fe_2O_3 content of 83% by mass and a Si/Al ratio of 2.7 (Herpi et al., 2021), $ZrOCl_2.8H_2O$ (Merck), NaOH (Merck), KH_2PO_4 (Merck), HCl (Merck), mineralized water, ammonium molybdate $(NH_4)_6Mo_7O_{24}$) (Merck), potassium antimonyl tartrate solid ($K_2Sb_2(C_4H_2O_6)_2$) (Merck), H_2SO_4 (Merck), and ascorbic acid ($C_8H_8O_6$) (Merck). The instruments were used in this research were UV-Vis 2450 Shimadzu spectrophotometer, Fourier Tansform Infrared (FTIR) Perkin Elmer Frontier Optica, Panalytical Epsilon1 X-Ray Fluoresence (XRF), Panalytical Xpert Pro X-Ray Diffraction (XRD) X-Pert3 Pro Material, FEI Quanta 650 Scanning Electron Microscopy (SEM) and Quantachrome Quadrawin Brunauer-Emmett-Teller (BET).

Fly Ash (FA) Preparation as Zeolite Raw Material (Herpi *et al.*, 2021)

The fly ash was filtered to a particle size of 80, oven-dried at 150 °C for four hours, and afterwards characterized using X-ray fluorescence (XRF). The fly ash was washed with 20% HCl (a solid-to-liquid ratio of 1:10), neutralized, and dried at 80 °C. Using Fourier transform infrared (FTIR) and X-ray diffraction (XRD), the samples of fly ash were characterized.

Synthesis of Fly Ash Zeolite (FAZ) (Rayalu *et al.*, 2000).

Fly ash (10 g) and NaOH (12 g) were mixed together and put together, then placed in a stainless-steel crucible and heated at 550 °C for two hours. In addition, the suspension was stirred magnetically for 24 hours while 100 mL of mineral water was added. The hydrothermal process was conducted in a Teflon autoclave at 100 °C for 24 hours. The obtained product was then washed with mineralized water until the pH of it was neutral and then dried. Finally, Characterizing the synthesized zeolites using FTIR, XRD, SEM, and BET.

Synthesis of Zirconium Modified Zeolite (ZrMZ)

Zirconium oxychloride octahydrate ($ZrOCl_2.8H_2O$) (5 g) was dissolved in 100 mL of mineralized water, and 10 g of fly ash zeolite (FAZ) was added. Then, the suspension was stirred magnetically for 24 hours. After that, 1 M NaOH solution was added gradually into the suspension until the pH was 10. Then, it was stirred magnetically for 1 hour. ZrMZ was separated by centrifugation, washed and dried at 105 °C (Yang *et al.*, 2014). Furthermore, it was characterized using FTIR, XRD, SEM, and BET.

Phosphate Adsorption Analysis by FA, FAZ, and ZrMZ

FA, FAZ, and ZrMZ were dispersed in 25 mL of a 3 mg/L phosphate solution. The mixture was magnetically stirred for 60 minutes, then set aside for 90 minutes before filtering using Whattman filter paper number 42. After that, 10 mL of sample was taken, and one drop of phenolphthalein indicator was added. If a pink color emerges, 5N H_2SO_4 is added until the color vanishes. In addition, 3.2 mL of molybdenum blue solution was added. The mixture was homogenized and left to stand

for 15 minutes. The mixture's absorbance was measured at 800-900 nm. Equation 1 can be used to compute the equilibrium zeolite's adsorption capacity. Meanwhile, the phosphate adsorption efficiency is estimated using equation 2. The effect of adsorbent dosage was investigated at adsorbent dosage of 0.025, 0.050, 0.075, 0.100, 0.125, and 0.150 grams; the effect of pH was investigated at pH of 3, 5, 7, 9, and 11, and the effect of contact time was investigated at contact time of 15, 30, 60, 90, and 120 minutes.

$$\text{Qe (mg/g)} = \frac{[(Co-Ce).V]}{m} \quad (1)$$

$$\text{Adsorption efficiency (\%)} = \frac{Co-Ce}{Ce} \text{ x } 100\% \quad (2)$$

where Qe is the amount of metal ions adsorbed onto a unit mass of adsorbent (mg metal ions/g adsorbent) at equilibrium; Co and Ce are the concentrations of metal ions in the initial solution and in the aqueous phase after treatment; m is the amount of adsorbent used (g); and V is the volume of solution (L).

Applications of Phosphate Adsorption by FA, FAZ, and ZrMZ in Aquatic Environment

Lake water was taken from Agathis Lake, University of Indonesia, on June 7, 2022, at 10.00 WIB at coordinates 6°22'06.6 "S" and 106°49'29.3 "E. The sampling method used in this study is the integrated place sample method, where samples from several specific points are taken with the same volume and time and then mixed in one container (Ahdiaty & Fitriana, 2020).

3. RESULTS AND DISCUSSIONS

The Characteristic of Fly Ash, FAZ, and ZrMZ

FT-IR characterization was performed on fly ash (FA), fused fly ash (FAL), fly ash zeolite (FAZ), and zirconium modified zeolite (ZrMZ) at a wavelength of 4000-400 cm^{-1}.

Figure 1 shows that there are absorption bands of FAZ and ZrMZ at 3479.73 and 3549.47 cm^{-1}, respectively, with quite strong intensity for FAZ, where these wavenumbers indicate O-H streaching vibrations (Byrappa, 2007). H-O-H bond bending vibrations for water molecules (H_2O) are shown at 168.03 cm^{-1} for FAL, 1639.56 cm^{-1} for FAZ, and 1645.35 cm^{-1} for ZrMZ with strong intensity. Asymmetry stretching vibration absorption bands of Si-O or Al-O in tetrahedral SiO_4 or AlO_4 appeared at 1053.17, 1003.99, 1001.09, and 992.41 cm^{-1} for FA, FAL, FAZ, and ZrMZ, respectively. These absorption bands correspond to Si/Al-O asymmetry stretching vibrations (Deng *et al.*, 2016; Safitri *et al.*, 2020). Absorption bands that indicate the presence of zeolite appear in the 500–420 cm^{-1} region (Jumaeri *et al.*, 2013). FAZ is observed at 462.93 cm^{-1}, and ZrMZ is found at 457.14 cm^{-1}, which is a T-O (Si/Al-O) bending vibration.

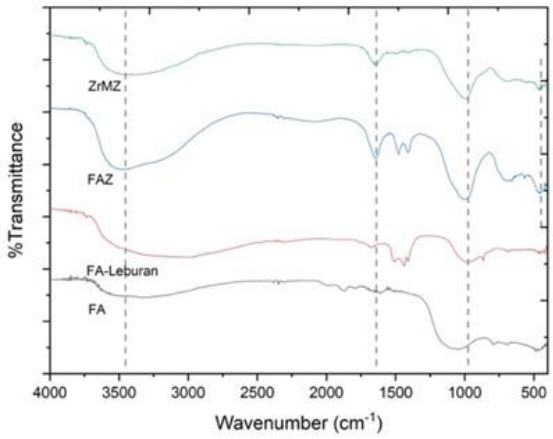

Figure 1. IR spectra of fly ash (FA), fused fly ash (FAL), fly ash zeolite (FAZ), and zirconium-modified zeolite (ZrMZ)

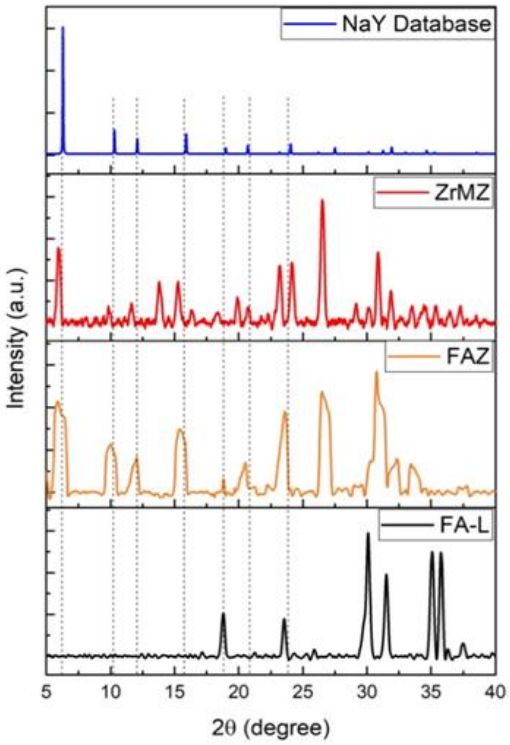

Figure 1. XRD spectrum of fused fly ash (FAL), fly ash zeolite (FAZ), and zirconium modified zeolite (ZrMZ)

The XRD spectrum of fused fly ash (FAL) from the fusion of fly ash with NaOH, fly ash zeolite (FAZ), and zirconium modified zeolite (ZrMZ) is shown in **Figure 2**. The FAZ peaks at 2θ of 6.12; 11.75; 18.47; 23.37; 26.71; and 37.44° appear to match the peak positions in the zeolite Na-Y database retrieved from IZA-Online, indicating that the fly ash synthesis was successful in generating Y-type zeolites according to JCPDS 96-231-1100 and ICSD 98-016-9077. The diffraction peak of zirconium oxide in the diffractogram of zirconium modified zeolite (ZrMZ) was not observed because the zirconium oxide in ZrMZ is amorphous (Yang *et al.*, 2015).

The morphology of fly ash (FA) displayed in **Figure 3a** is an amorphous aluminosilicate sphere, which is the primary form of morphology seen in fly ash (FA) (Herpi *et al.*, 2021). **Figure 3b** shows the morphology of FAZ, which consists of cubic crystalline particles that are nearly consistent in size and regular in shape. In contrast to the clearly evident FAZ morphology (**Figure 3b**), the morphology of ZrMZ in **Figure 3c** has a less distinct shape due to zirconium oxide particles adhered to the zeolite surface (Yang *et al.*, 2015). The EDAX spectra of FAZ revealed the presence of O, C, Si, Al, Na, Ca, and Fe elements on the FA surface, whereas ZrMZ revealed the presence of Zr, O, C, Si, Al, Na, Ca, and Fe elements. These SEM results confirmed the formation of a zirconium oxide layer on the fly ash zeolite after modification (Yang *et al.*, 2015).

The nitrogen adsorption-desorption isotherm graphs of FAZ and ZrMZ as determined by BET analysis are depicted in Figure 5a. The adsorption-desorption isotherm of FA adsorbent is a type II curve with a hysteresis loop at a P/P_0 of 0.20. FA adsorbent had an S_{BET} of 8.13 m^2/g (Herpi *et al.*, 2021). The FAZ adsorbent displays a type IV curve with a hysteresis loop at a P/P_0 of 0.90, which indicates that it is a mesoporous zeolite. Brunauer-Emmett-Teller (S_{BET}) of FAZ is 51.35 m^2/g, which is significantly less than the S_{BET} value of 626 m^2/g for commercial Na-Y zeolite. Due to the fact that the primary source material for this synthesis is natural material, it is conceivable that the synthesized zeolite contains numerous impurities and other elements. The ZrMZ adsorbent displayed a type IV curve with a relatively large hysteresis loop at P/P_0 0.4, indicating that the zeolite is mesoporous, and the S_{BET} value increased to 384.95 m^2/g (**Table 1**).

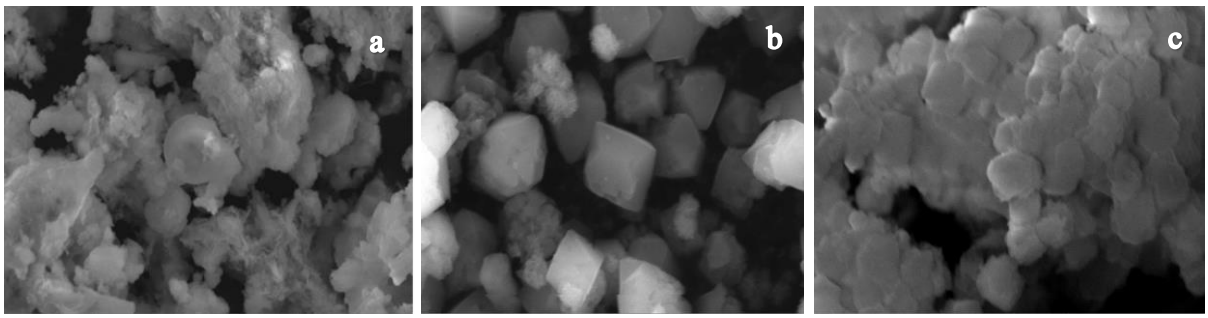

Figure 2. The morphology of (a) FA, (b) FAZ, and (c) ZrMZ

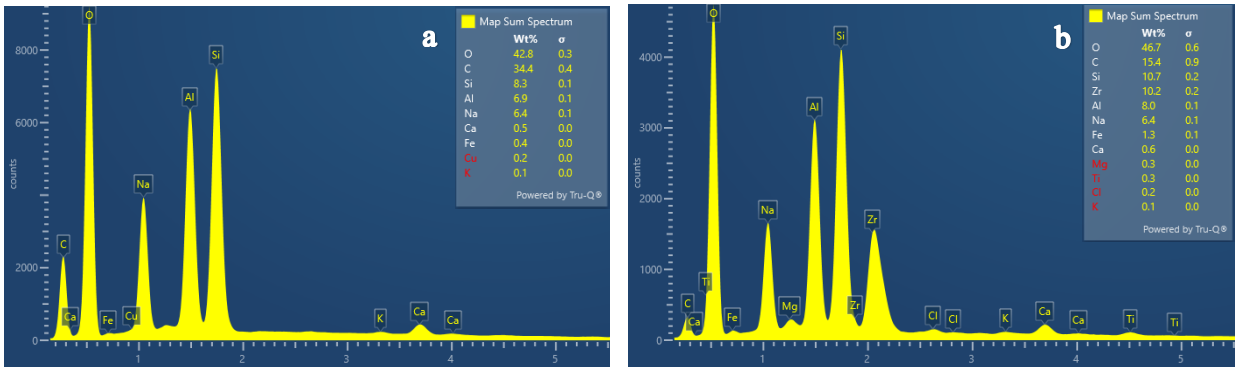

Figure 3. The EDAX spectrum of (a) FAZ and (b) ZrMZ

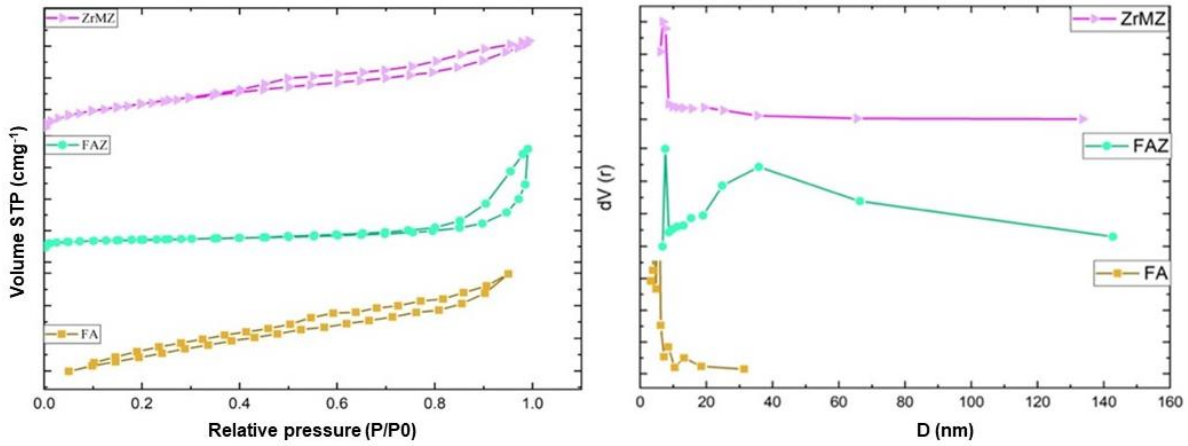

(a) (b)

Figure 4. (a) Adsorption-desorption isotherms of FA, FAZ, and ZrMZ, (b) Pore size distribution of FA, FAZ, and ZrMZ by BJH desorption method.

Table 1. Surface area and pore volume of FA, FAZ, and ZrMZ

Material	S_{BET}[a] m^2/g	S_{ext}[b] m^2/g	S_{mic}[b] m^2/g	V_{tot}[c] cm^3/g	V_{micro}[b] cm^3/g	V_{meso}[b] cm^3/g
FA*	8.135	3.772	4.363	7.843×10^{-3}	6.0×10^{-3}	1.843×10^{-3}
FAZ	51.3577	44.7402	6.6174	0.1054	0.0046	0.1007
ZrMZ	384.9555	135.764	249.191	0.3223	0.1004	0.3176

*(Herpi *et al.*, 2021).

Figure 5b depicts the pore size distribution of FA, FAZ, and ZrMZ adsorbents as determined by the Barrett Joyner Halenda (BJH) desorption procedure. The pore size distributions of FA, FAZ, and ZrMZ are, respectively, 3.27, 7.63, and 6.85 nm. IUPAC classifies porous materials into three categories based on their pore diameter: microporous materials with a pore diameter of 2 nm, mesoporous materials with a pore diameter of 2–50 nm, and macroporous materials with a pore diameter of > 50 nm (Salehi *et al.*, 2020). Therefore, FA, FAZ, and ZrMZ adsorbents are mesoporous substances. by pore filling, demonstrating that Zr molecules have filled the pore volume (Salehi *et al.*, 2020).

Effect of Adsorbent Dosage on Phosphate Adsorption Capacity

The effect of the adsorbent dosages on the adsorption process is carried out because it is directly related to the number of active sites available in the phosphate absorption process, so that the optimum number of adsorbents can be known when achieving the highest adsorption efficiency (Aryee *et al.*, 2021).

Figure 6 shows an increase in adsorption efficiency as the adsorbent dosage increases. At 0.150 g of adsorbent, the adsorption efficiency was 27.56%. Fly ash zeolite (FAZ) at 0.125 g produced the highest adsorption efficiency of 50.62%. Meanwhile, the highest adsorption efficiency on ZrMZ was formed when the adsorbent dosage was 0.75 g, with an adsorption efficiency of 99.51%. The higher FAZ and ZrMZ adsorbent dosage resulted in a decreased adsorption efficiency due to the uptake of phosphate ions at equilibrium not increasing significantly as the adsorbent dosage increased because the saturation level had been reached during the adsorption process (Ragheb, 2013).

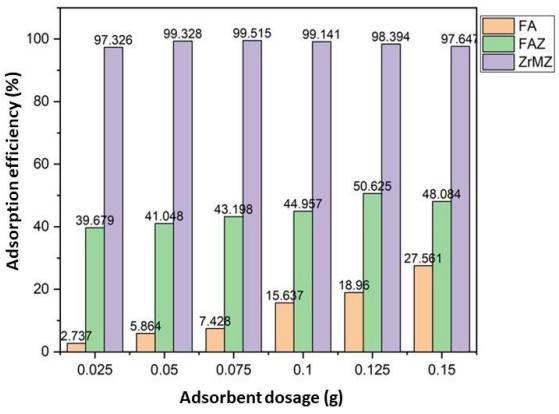

Figure 5. Phosphate adsorption efficiency with varying of adsorbent dosages

Effect of pH on Phosphate Absorption

The pH value of the phosphate solution was adjusted using 0.1 M HCl and 0.1 M NaOH

until the pH was suitable and stable during the adsorption process. Fly ash adsorbent (FA) was optimum at pH 3, with an adsorption capacity of 0.341 mg/g. The highest adsorption capacity result for FAZ was 0.522 mg/g, where the optimum pH was pH 7. The highest adsorption capacity for ZrMZ was at pH 7, with a value of 0.956 mg/g (**Figure 7**).

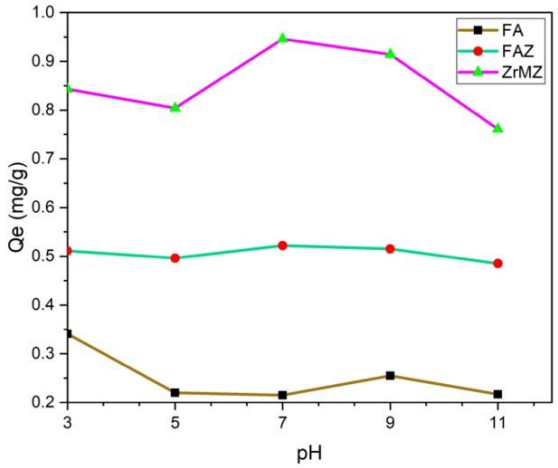

Figure 6. The adsorption capacity of an adsorbent on pH variation

A higher pH decreased the adsorption capacity. Because of the repulsion between the negatively charged adsorbent surface and negatively charged phosphate ions. At low to neutral pH, the adsorbent surface is positively charged, and electrostatic attraction between negatively charged phosphate anions and the positively charged adsorbent surface increases phosphate adsorption (Chitrakar *et al.*, 2006). The decrease in phosphate uptake in the pH > 7 region may be due to the surface charge of the adsorbent becomes more negative with increasing pH, triggering a greater electrostatic repulsive force towards the more negatively charged phosphate anions, namely HPO_4^{2-} and PO_4^{3-} (Chitrakar *et al.*, 2006).

Effect of Contact Time on Phosphate Adsorption

The effect of contact time on phosphate absorption using FA, FAZ, and ZrMZ adsorbents can be seen in **Figure 8**. FA adsorbent showed the optimum adsorption capacity at 90 minutes, with an adsorption capacity of 0.428 mg/g. FAZ and ZrMZ produced optimum contact time at 60 minutes, with the highest adsorption capacities for FAZ and ZrMZ being 0.548 and 0.943 mg/g, respectively. The adsorption rate decreased at a later stage due to the slow pore diffusion of dissolved ions into the bulk of the adsorbent (Ragheb, 2013).

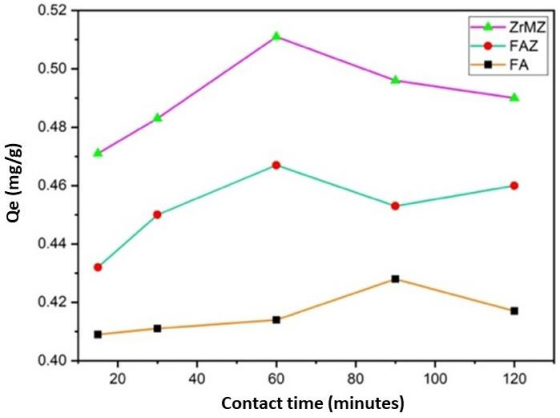

Figure 7. The adsorption capacity of adsorbent at several contact times

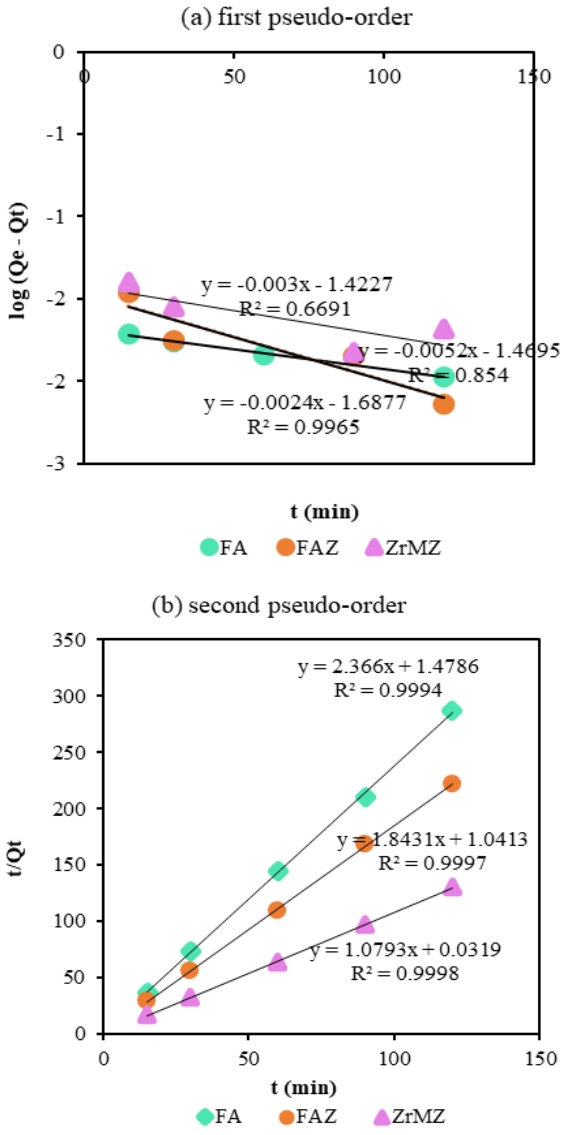

Figure 8. Linear regression of adsorption kinetics (a) first pseudo-order and (b) second pseudo-order

A model of adsorption kinetics was used to determine the relationship between the adsorbate removal rate and the adsorbate concentration during the adsorption process (Isiuku *et al.*, 2021). Simulating the experimental data using first- and second-order pseudo-order models. The first pseudo-order involves surface active sites and affinity, while the second pseudo-order involves valence forces and electron exchange between the adsorbent and the adsorbate (Zhang *et al.*, 2022).

The adsorption kinetics of the three adsorbents showed that the first pseudo-order equation was not sufficient to describe the interaction mechanism between adsorbent and phosphate (**Figure 9a**), while the second pseudo-order described the chemical adsorption between adsorbent and phosphate with the R^2 values of 0.9994, 0.9997, and 0.9998 for FA, FAZ, and ZrMZ, respectively (**Figure 9b**). The first pseudo-order implies that one adsorbate (PO_4^{3-}) can be adsorbed onto one sorbent surface site, while the second pseudo-order adsorption kinetic rate model indicates that chemical sorption is the rate controller in the adsorption process (Li *et al.*, 2016). The regression coefficient of the second all-order model was declared to be the best kinetic model (R^2 = 0.9980) of phosphate sorption by an iron oxide-based sorbent (Lalley *et al.*, 2016). Zhang *et al.* (2022) stated that pseudo-second-order kinetics generally fit the experimental data better for metal-based composite adsorption systems, as they describe the binding between phosphate and sorbent that depends on complex chemisorption.

Field Application

Measurement of the adsorption capacity and adsorption efficiency of FA, FAZ, and ZrMZ on lake water was carried out under conditions that were adjusted to the optimum results of the three adsorbent materials using the batch method. Lake water sampling was carried out at four points, each of which took 25 mL of lake water. When taking lake water, the temperature and pH of the water were also measured. Measurement of adsorption capacity and adsorption efficiency was carried out on lake water with the temperature and pH of the lake water and the optimum adsorbent dosage and contact time of each adsorbent. **Table 2** shows the temperature and pH data at the time of lake water sampling.

Table 2. Sampling data at Agathis Lake, University of Indonesia

Parameter	Point 1	Point 2	Point 3	Point 4
Temperature (ºC)	29	31	29	33
pH	7.95	7.39	7.6	7.03

Table 3 shows the adsorption capacity and adsorption efficiency of phosphate by FA, FAZ, and ZrMZ measured using a UV-Vis spectrophotometer. The highest adsorption capacity and adsorption efficiency were obtained by ZrMZ adsorbent, with an adsorption capacity of 0.186 mg-P/g and an efficiency of phosphate adsorption of 81.137%.

Table 3. Adsorption capacity and adsorption efficiency of phosphate by FA, FAZ, and ZrMZ

Material	Qe (mg/g)	Adsorption efficiency (%)
FA	0.073	64.083
FAZ	0.109	79.070
ZrMZ	0.186	81.137

Zirconium-modified fly ash zeolite (ZrMZ) is very effective as an adsorbent for phosphate absorption in water. ZrMZ adsorbent is optimum at 0.075 g, pH 7, and a contact time of 60 minutes. Research by K. Zhang et al. (2021) reported that zeolites from fly ash can adsorp the phosphate ion with a phosphate adsorption capacity of 84.4 mg/g in wastewater that has a phosphate concentration of 8,000 mg/L and pH 1.78.

4. CONCLUSIONS

Fly ash (FA), fly ash zeolite (FAZ), and zirconium modified zeolite (ZrMZ) were used as phosphate adsorbents in aquatic systems. Adsorbent type, pH, and contact time had an impact on the adsorption capacity. The adsorption process was more effective at pH 5 for FA adsorbents and pH 7 for FAZ and ZrMZ adsorbents, with a contact time of 90 min for FA and 60 min for FAZ and ZrMZ. The adsorption kinetics model for FAZ and ZrMZ followed the second pseudo-order model. The three adsorbents, FA, FAZ, and ZrMZ, were tested on lake water samples obtained from Agathis Lake, University of Indonesia. ZrMZ successfully adsorbed phosphate the best among other adsorbents, with an adsorption capacity of 0.186 mg-P/g and an adsorption efficiency of 81.137%.

REFERENCES

Ahdiaty, R., & Fitriana, D. (2020). Pengambilan Sampel Air Sungai Gajah Wong di Wilayah Kota Yogyakarta. *IJCA (Indonesian Journal of Chemical Analysis)*, *3*(2), 65–73. https://doi.org/10.20885/ijca.vol3.iss2.art4

Aryee, A. A., Dovi, E., Shi, X., Han, R., Li, Z., & Qu, L. (2021). Zirconium and iminodiacetic acid modified magnetic peanut husk as a novel adsorbent for the sequestration of phosphates from solution: Characterization, equilibrium and kinetic study. *Colloids and Surfaces A: Physicochemical and Engineering Aspects*, *615*. https://doi.org/10.1016/j.colsurfa.2021.126260.

Byrappa, K. (2007). Characterization of zeolites by infrared spectroscopy Triazole derivatives View project Microwave Assisted Synthesis and Characterization of Nanostructure Zinc Oxide-Graphene Oxide and Photo Degradation of Brilliant Blue View project. In *Article in Asian Journal of Chemistry*. https://www.researchgate.net/publication/283862901.

Chitrakar, R., Tezuka, S., Sonoda, A., Sakane, K., Ooi, K., & Hirotsu, T. (2006). Selective adsorption of phosphate from seawater and wastewater by amorphous zirconium hydroxide. *Journal of Colloid and Interface Science*, *297*(2), 426–433. https://doi.org/10.1016/j.jcis.2005.11.011.

Deng, L., Xu, Q., & Wu, H. (2016). Synthesis of Zeolite-like Material by Hydrothermal and Fusion Methods Using Municipal Solid Waste Fly Ash. *Procedia Environmental Sciences*, *31*, 662–667. https://doi.org/10.1016/j.proenv.2016.02.122.

Dwi Jananti, P., Kusumastuti Jurusan Kimia, E., & Matematika dan Ilmu Pengetahuan Alam, F. (n.d.). *Sintesis Zeolit A Dari Abu Layang Batubara Melalui Modifikasi Proses Hidrotermal*.

Faradilla, A. R., Yulinawati, H., Suswantoro, E., Lingkungan, J. T., Lansekap, A., & Lingkungan, T. (2016). Pemanfaatan Fly Ash Sebagai Adsorben Karbon Monoksida Dan Karbon Dioksida Pada Emisi Kendaraan Bermotor. *Seminar Nasional Cendekiawan*.

Goscianska, J., Ptaszkowska-Koniarz, M., Frankowski, M., Franus, M., Panek, R., & Franus, W. (2018). Removal of phosphate from water by lanthanum-modified zeolites obtained from fly ash. *Journal of Colloid and Interface Science*, *513*, 72–81. https://doi.org/10.1016/j.jcis.2017.11.003.

Herpi, A., Yunarti, R., & Saefumillah, A. (2021, October 19). *Synthesized Zeolite from Coal Fly Ash: Effect of Furnace and Acidic Pretreatment on the Characteristic*. https://doi.org/10.4108/eai.19-12-2020.2309115.

Isiuku, B. O., Enyoh, C. E., Duru, C. E., & Ibe, F. C. (2021). Phosphate ions removal from aqueous phase by batch adsorption on activated (activation before carbonization) biochar derived from rubber pod husk. *Current Research in Green and Sustainable Chemistry*, *4*. https://doi.org/10.1016/j.crgsc.2021.100136.

Jumaeri, Jananti, P. D., & Kusumastuti, E. (2013). *Sintesis Zeolit A Dari Abu Layang Batubara Melalui Modifikasi Proses Hidrotermal*.

Lalley, J., Han, C., Li, X., Dionysiou, D. D., & Nadagouda, M. N. (2016). Phosphate adsorption using modified iron oxide-based sorbents in lake water: Kinetics, equilibrium, and column tests. *Chemical Engineering Journal*, *284*, 1386–1396. https://doi.org/10.1016/j.cej.2015.08.114.

Li, M., Liu, J., Xu, Y., & Qian, G. (2016). Phosphate adsorption on metal oxides and metal hydroxides: A comparative review. In *Environmental Reviews* (Vol. 24, Issue 3, pp. 319–332). Canadian Science Publishing. https://doi.org/10.1139/er-2015-0080.

Ma, H., Zhang, J., Wang, M., & Sun, S. (2019). Modification of Y-Zeolite with Zirconium for Enhancing the Active Component Loading: Preparation and Sulfate Adsorption Performance of ZrO(OH)2/Y-Zeolite. *ChemistrySelect*, *4*(27), 7981–7990. https://doi.org/10.1002/slct.201901519.

Patty, S. I. (2014). Characteristics of Phosphate, Nitrate and Dissolved Oxygen in Gangga and Siladen Island Waters, North Sulawesi. *Jurnal Ilmiah Platax*, *2*(2). http://ejournal.unsrat.ac.id/index.php/platax.

Poernomo, H., Biyantoro, D., & MariaVeronica Purwani Pusat Teknologi Akselerator dan Proses Bahan -BATAN Jalan Babarsari Kotak Pos, dan. (n.d.). *Kajian Konsep Teknologi Pengolahan Pasir Zirkon Lokal Yang Mengandung Monasit, Senotim, Dan Ilmenit*,

The Concept Study Of Processing Technology Of Local Zircon Sand Containing Monazite, Xenotime, And Ilmenite.

Ragheb, S. M. (2013). Phosphate removal from aqueous solution using slag and fly ash. *HBRC Journal*, *9*(3), 270–275. https://doi.org/10.1016/j.hbrcj.2013.08.005.

Rayalu, S., Meshram, S. U., & Hasan, M. Z. (2000). Highly crystalline faujasitic zeolites from flyash. In *Journal of Hazardous Materials* (Vol. 77). www.elsevier.nlrlocaterjhazmat.

Rodrigues, L. A., Maschio, L. J., Coppio, L. D. S. C., Thim, G. P., & da Silva, M. L. C. P. (2012). Adsorption of phosphate from aqueous solution by hydrous zirconium oxide. *Environmental Technology (United Kingdom)*, *33*(12), 1345–1351. https://doi.org/10.1080/09593330.2011.632651.

Safitri, L. E., Zuryati, U. K., Rohma, H. N., Ni'Mah, Y. L., & Prasetyoko, D. (2020). Synthesis zeolite y from kaolin bangka belitung: Activation of metakaolin with various concentration of sulfuric acid. *Journal of Physics: Conference Series*, *1567*(3). https://doi.org/10.1088/1742-6596/1567/3/032099.

Salehi, S., Alijani, S., & Anbia, M. (2020). Enhanced adsorption properties of zirconium modified chitosan-zeolite nanocomposites for vanadium ion removal. *International Journal of Biological Macromolecules*, *164*, 105–120. https://doi.org/10.1016/j.ijbiomac.2020.07.055.

Sasongko, E. B., Widyastuti, E., & Priyono, R. E. (2014). *Kajian Kualitas Air Dan Penggunaan Sumur Gali Oleh Masyarakat Di Sekitar Sungai Kaliyasa Kabupaten Cilacap*. *12*, 72–82.

Simbolon, A. R. (n.d.). *Pencemaran Bahan Organik dan Eutrofikasi di Perairan Cituis, Pesisir Tangerang*.

Xiong, W., Tong, J., Yang, Z., Zeng, G., Zhou, Y., Wang, D., Song, P., Xu, R., Zhang, C., & Cheng, M. (2017). Adsorption of phosphate from aqueous solution using iron-zirconium modified activated carbon nanofiber: Performance and mechanism. *Journal of Colloid and Interface Science*, *493*, 17–23. https://doi.org/10.1016/j.jcis.2017.01.024.

Yang, M., Lin, J., Zhan, Y., & Zhang, H. (2014). Adsorption of phosphate from water on lake sediments amended with zirconium-modified zeolites in batch mode. *Ecological Engineering*, *71*, 223–233. https://doi.org/10.1016/j.ecoleng.2014.07.035.

Yang, M., Lin, J., Zhan, Y., Zhu, Z., & Zhang, H. (2015). Immobilization of phosphorus from water and sediment using zirconium-modified zeolites. *Environmental Science and Pollution Research*, *22*(5), 3606–3619. https://doi.org/10.1007/s11356-014-3604-2.

Zahrah, N., Saefumillah, A., & Yunarti, R. T. (2020). Study of phosphate adsorption from aquatic system using fly ash residue modified with magnetite (Fe_3O_4). *AIP Conference Proceedings*, *2242*. https://doi.org/10.1063/5.0010656.

Zhang, K., van Dyk, L., He, D., Deng, J., Liu, S., & Zhao, H. (2021). Synthesis of zeolite from fly ash and its adsorption of phosphorus in wastewater. *Green Processing and Synthesis*, *10*(1), 349–360. https://doi.org/10.1515/gps-2021-0032.

Zhang, P., He, M., Huo, S., Li, F., & Li, K. (2022). Recent progress in metal-based composites toward adsorptive removal of phosphate: Mechanisms, behaviors, and prospects. *Chemical Engineering Journal*, *446*, 137081. https://doi.org/10.1016/j.cej.2022.137081.